Springer

Journal of Mechanical Science and Technology 23 (2009) 2059~2071

Journal of Mechanical Science and Technology

www.springerlink.com/content/1738-494x
DOI 10.1007/s12206-009-0506-1

Development of an aircraft worst case flutter prediction with Mach variation using robust stability analysis †

Chan Hoon Chung[1], Sang Joon Shin[1,*] and Taehyoun Kim[2]

[1]*Graduate Student, School of Mechanical and Aerospace Engineering, Seoul National University, 56-1 Shillim-dong, Kwanak-gu, Seoul 151-744, Korea*

[2]*Principal Engineer, Loads and Dynamics, Boeing Commercial Company, Seattle, WA 98124-2207, U.S.A.*

(Manuscript Received April 29, 2008; Revised January 21, 2009; Accepted April 28, 2009)

Abstract

Modern aircraft are under a severe operating environment, in which uncertainties in mass, stiffness, and aerodynamic characteristics could play an important role in determining the safety of an airplane. Recently, several analysis methodologies have been proposed to find a new critical flight condition in the presence of the system uncertainties. In the present paper, a variation is assumed to exist in the aerodynamic characteristics. A robust aeroelastic analysis is established which accounts for aerodynamic variation due to a different level of compressibility and atmospheric density. Mathematically, the variations in Mach number and atmospheric density are treated as aerodynamic uncertainties. A robust flutter stability boundary is obtained by using the mu method. It is found that the worst case flutter speed, dynamic pressure, and atmospheric density results are all more conservative than the nominal flutter results.

Keywords: Robust aeroelasticity; Flutter; Worst case flutter boundary; Mu method; Unsteady aerodynamics; Doublet lattice method

1. Introduction

The modern aircraft, especially those used for military operations, is generally required to have high performance and maneuverability to accomplish the complicated mission in a severe environment. In general, there exist limitations today in predicting the performance and safety of those aircraft with reliable accuracy and confidence. The aeroelastic phenomenon known as flutter is one of the critical factors which limit the aircraft flight speed and performance. Furthermore, when the aircraft is in a wartime operation, there exist many factors which give rise to an uncertainty in the critical flight condition, i.e., the flutter speed. For instance, fuel consumption during the flight generates a variation in mass of either the wing or a pylon causing a change in wing structural modes, and subsequently in its corresponding aerodynamic forces. Such a variation ultimately will affect the flutter stability boundary characteristics of the aircraft. Thus, an accurate estimation of the flutter stability, which takes such possible variations into account, is essential for predicting and guaranteeing a robust aircraft flight envelope. Recently, a few investigators have proposed a systematic way to find the variation of the aircraft flutter boundary using the concept of uncertainty. Livne reported that such a systematic way regarding uncertainties would be one of the important branches in future investigation in the field of aeroelasticity [1]. Lind suggested a match point solution methodology regarding the worst case flutter stability prediction [2]. In his analysis, generalized aerodynamic forces were obtained by DLM and RFA method was applied to convert them to state-space format. To account for aerodynamic uncertainty, Lind introduced a bounded uncertainty within the

† This paper was recommended for publication in revised form by Associate Editor Hong Hee Yoo

*Corresponding author. Tel.: +82 2 880 1642, Fax.: +82 2 887 2662
E-mail address: ssjoon@snu.ac.kr

© KSME & Springer 2009

poles of RFA formulation. Borglund suggested the so-called μ -k method for the robust aeroelastic stability analysis [3]. In his analysis, frequency-domain aeroelastic stability analysis was conducted with a local variation of pressure coefficient on a lifting surface. An uncertainty in pressure coefficients was assumed to exist near the wing tip and nacelle. DLM was also used to model the aerodynamic loads. Both researchers considered a constant Mach problem. Danowsky adopted a similar flutter prediction method for a more practical two-dimensional wing [10] by using a NASTRAN structural model and doublet lattice aerodynamics [11]. However, his method required a large number of discretized panels to guarantee accuracy of the analysis.

In the present paper, a brand new flutter analysis methodology that accounts for variations in both the unsteady compressible effect and altitude is introduced. Generalized mass, stiffness matrices, and aerodynamic forces are formulated based on the work by Hodges [6]. The present method is an extension from the classical methodology which has been used for a two-dimensional airfoil, where Theodorsen's lift deficiency function is defined and used to find general aerodynamic lift and moment for arbitrary motions. A new aerodynamic modeling methodology is suggested based on this type of aeroelastic formulation. For nominal flutter prediction, a numerical analysis based on varying altitude and flight speed problem is solved under an initial Mach number, where the mu method is invoked with the altitude as sole uncertainty parameter. A corresponding match point problem is also taken into account. When an initial Mach number and an initial atmospheric density are prescribed, robust flutter stability boundary is obtained by the mu method. In that case, the flutter speed and dynamic pressure are related by altitude because the atmospheric density and temperatures are changed.

For the present robust flutter analysis, the lower and upper bounds of Mach number and atmospheric density variation are prescribed. The boundaries of the altitude and speed are prescribed by the weighting values. The variation of Mach number is obtained from the aerodynamic state matrix. The corresponding weighting matrix is obtained from difference between the lower and upper values of the aerodynamic state matrix. Then, these variation models are accounted for as the uncertainty in the mu method.

Approximation on Theodorsen's lift deficiency function is obtained by DLM and its result is compared with the original Theodorsen's result [5, 12]. Theodorsen's lift deficiency functions corresponding to different Mach numbers are also obtained, and the nominal flutter speed is predicted for each altitude and Mach number. The variation boundaries of the aerodynamic characteristics are selected from these lift deficiency functions for the different Mach numbers. Finally, a worst case flutter stability boundary result for a three-dimensional wing is presented, which is based on the mu method. The robust aeroelastic analysis results are compared with those obtained from the nominal stability analysis.

2. Aeroelastic system of a three-dimensional wing

2.1 Three-dimensional wing

Fig. 1 represents a general three-dimensional wing that is analyzed as a cantilevered beam. This wing is an unswept rectangular wing, and hence it allows one to use uncoupled mode shapes represented by trigonometric and hyperbolic functions to approximate the coupled bending and torsional mode shapes. Aerodynamically, the wing will be assumed to be a flat plate, so, thickness and camber effects will be neglected henceforth.

2.2 Structural and aerodynamic models of the three-dimensional wing

An aeroelastic equation for the present three-dimensional wing may be expressed as follows, based on the equations used in a general mechanical vibration problem.

$$M\ddot{q} + Kq = F_G \tag{1}$$

Starting from Eq. (1), the foregoing derivations are based on the work by Hodges [6]. In the above equa-

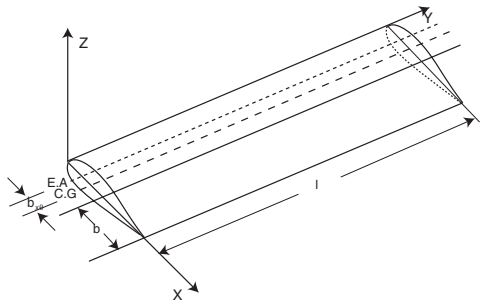

Fig. 1. A three-dimensional cantilevered wing.

tion, q is a state vector representing the generalized bending and torsional degrees of freedom described as follows.

$$q = \begin{bmatrix} \eta \\ \theta \end{bmatrix} \tag{2}$$

M and K denote the generalized mass and stiffness matrix, respectively.

$$M = ml \begin{bmatrix} [I] & -bx_\theta [A]^T \\ -bx_\theta [A] & b^2 r^2 [I] \end{bmatrix} \tag{3}$$

$$K = \begin{bmatrix} \dfrac{EI}{l^3}[B] & [0] \\ [0] & \dfrac{GJ}{l}[T] \end{bmatrix} \tag{4}$$

In the above equation, matrix A denotes a coupled modal effect, which is represented as

$$A_{ij} = \frac{1}{l}\int_0^1 \Theta_i \Psi_i dy \tag{5}$$

And matrices B and T are bending and torsion coefficients represented as

$$B_{ii} = (\alpha_i l)^4 \tag{6}$$

$$T_{ii} = (r_i l)^2 \tag{7}$$

Using a three-dimensional beam analysis model, the structure characteristic values could be obtained with one-dimensional beam method and two-dimensional cross section method. From these methods, the stiffness matrix can be obtained. Thus, the structure results obtained from Eqs. (3) and (4) will be compared with another structural result which is obtained from one-dimensional beam analysis and two-dimensional cross section analysis method. However, thickness effects are ignored in the present paper and need not be considered with these methods.

In Eq. (1), F_G is a generalized aerodynamic forcing vector which is based on structural mode shapes as follows.

$$F_G = \begin{bmatrix} \Xi_\omega \\ \Xi_\theta \end{bmatrix} \tag{8}$$

where Ξ_ω and Ξ_θ are the weighted aerodynamic forces, defined as

$$\Xi_{\omega_i} = \int_0^l \Psi_i L' dy \tag{9}$$

$$\Xi_{\theta_i} = \int_0^l \Theta_i \left[M'_{1/4} + (1/2 + a) b L' \right] dy \tag{10}$$

The aerodynamic forcing vector is now formulated in a matrix form as follows.

$$\begin{bmatrix} \Xi_\omega \\ \Xi_\theta \end{bmatrix} = -\pi\rho b^2 l \begin{bmatrix} [I] & ba[A]^T \\ ba[A] & b^2(a^2 + 1/8)[I] \end{bmatrix} \ddot{q}$$
$$-\pi\rho bUl \begin{bmatrix} 2C(k)[I] & -b[1 + 2(1/2 - a)C(k)][A]^T \\ 2b(1/2 + a)C(k)[A] & b^2(1/2 - a)[1 - 2(1/2 + a)C(k)][I]] \end{bmatrix} \dot{q}$$
$$-\pi\rho bU^2 l \begin{bmatrix} [0] & -2C(k)[A]^T \\ [0] & -b(1 + 2a)C(k)[I] \end{bmatrix} q \tag{11}$$

Two kinds of aerodynamic models will be used. The first is a full blown unsteady aerodynamics which uses both the circulatory and non-circulatory part in lift and pitching moment. The second one contains the circulatory lift only. In the foregoing numerical analysis, both aerodynamic models will be used in the nominal flutter analysis. In the robust analysis, results will be obtained with the circulatory part only.

3. Doublet lattice method and rational funtion approximation

3.1 Doublet lattice method (DLM)

DLM is used for estimating accurate unsteady aerodynamic forces acting on the present three-dimensional wing. In this process, the cantilevered wing is assumed as a flat plate. Specifically, its governing equation is a linearized small disturbance velocity potential equation including compressibility [11]. In DLM, the continuous pressure doublet sheet is replaced by a discrete doublet line [11].

In Fig. 2, the dotted line denotes an aerodynamic center which lies on a quarter chord point of each panel and the circles are doublet lattice points located on the third quarter point of each panel. An indicial lift is obtained by the present DLM analysis and then the range of the variation due to uncertainty is estimated. Finally, the generalized aerodynamic force is obtained in terms of the change in the mode shape and natural frequencies. Simultaneously, in order to extract Theodorsen's lift deficiency function which is originally defined for a two-dimensional airfoil, a

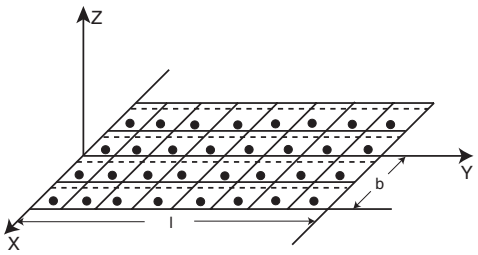

Fig. 2. Wing dscretization used in DLM analysis.

three-dimensional wing with an intentionally exaggerated aspect-ratio is analyzed by the present DLM procedure in the present paper.

3.2 Rational function approximation (RFA)

By a rational function approximation, Theodorsen's lift deficiency function can be transformed into an aerodynamic state-space form as follows.

$$\begin{aligned} \dot{x} &= A_{Q_0} x + B_{Q_0} u \\ y &= C_{Q_0} x + D_{Q_0} u \end{aligned} \tag{12}$$

where

$$x = \begin{bmatrix} \bar{x} \\ \bar{\bar{x}} \end{bmatrix} \tag{13}$$

$$u = \begin{bmatrix} \bar{w} \\ \bar{\bar{w}} \end{bmatrix} \tag{14}$$

The present state-space form is obtained to represent the lift deficiency function corresponding to a different flight Mach number. In Equation (12), x is an augmented state variable and u is a generalized upwash input variable, in which the relevant components are defined as follows.

$$\bar{w} = \int_0^1 \Psi u_2 dy \tag{15}$$

$$\bar{\bar{w}} = \int_0^1 \Theta u_2 dy \tag{16}$$

where u_2 is an original upwash which is defined and used in a general two-dimensional airfoil. Above new definitions are used instead of the general upwash for a two-dimensional airfoil in order to comply with the generalized aerodynamic forces given by Eqs. (9) and (10). It is noted that each upwash component has a numerical value different from that for the original upwash, because the structural mode shape is now included in the expressions. Eqs. (15) and (16) can be expressed as linear combinations of the generalized displacements and velocities as follows.

$$\begin{bmatrix} \bar{w} \\ \bar{\bar{w}} \end{bmatrix} = \begin{bmatrix} [I] & -b\left(\frac{1}{2}-a\right)[A]^T \\ b\left(\frac{1}{2}+a\right)[A] & -b^2\left(\frac{1}{2}-a\right)\left(\frac{1}{2}+a\right)[I] \end{bmatrix} \begin{bmatrix} \dot{\eta} \\ \dot{\phi} \end{bmatrix} + \begin{bmatrix} [0] & -U[A]^T \\ [0] & -b(1+2a)U[I] \end{bmatrix} \begin{bmatrix} \eta \\ \phi \end{bmatrix} \tag{17}$$

4. Mathematical model of an aeroelastic system

By observing Eq. (11), Theodorsen's lift deficiency function $C(k)$ may now be replaced by the following expression.

$$C(k) = \left\{ -1 + b\left(\frac{1}{2}+a\right) + U \right\} \times C_{Q_0} x + D_{Q_0} u_2 \tag{18}$$

Then, the resulting generalized aerodynamic force can be formulated as

$$\begin{aligned} \Xi_\omega &= -\pi\rho b^2 l\{[I]\ddot{\eta} + ba[A]^T\ddot{\phi}\} \\ &-\pi\rho bUl2\{(C_{Q_0}x + D_{Q_0}\dot{\eta}) - b[A]^T\dot{\phi} \\ &-2b\left(\frac{1}{2}-a\right)[A]^T(C_{Q_0}x + D_{Q_0}\dot{\phi})\} \\ &-\pi\rho bU^2 l(-2)(C_{Q_0}x + D_{Q_0}\phi)[A]^T \end{aligned} \tag{19}$$

$$\begin{aligned} \Xi_\theta &= -\pi\rho b^2 l\{ba[A]\ddot{\eta} + b^2\left(a^2 + \frac{1}{8}\right)[I]\ddot{\phi}\} \\ &-\pi\rho bUl\{2b\left(\frac{1}{2}+a\right)(C_{Q_0}x + D_{Q_0}\dot{\eta})[A] \\ &+b^2\left(\frac{1}{2}-a\right)[I]\dot{\phi} - 2b^2\left(\frac{1}{2}-a\right)\left(\frac{1}{2}+a\right)(C_{Q_0}x + D_{Q_0}\dot{\phi})\} \\ &-\pi\rho bU^2 l(-b)(1+2a)(C_{Q_0}x + D_{Q_0}\phi) \end{aligned} \tag{20}$$

The original aeroelastic equation, Eq. (1), is now rewritten as follows, reflecting all the derivations so far.

$$M\ddot{q} + kq = A_M\ddot{q} + A_C\dot{q} + A_K q + A_G x \tag{21}$$

The final aeroelastic equation in a state-space form is now derived as follows.

$$\begin{bmatrix} \dot{q} \\ \ddot{q} \\ x \end{bmatrix} = \begin{bmatrix} 0 & I \\ [M - A_M]^{-1} \times [A_K - K] & [M - A_M]^{-1} \times [A_C] \\ B_2 & B_1 \end{bmatrix}$$

$$\begin{bmatrix} 0 \\ [M-A_M]^{-1}\times[A_G] \\ A_{Q_0} \end{bmatrix} \begin{bmatrix} q \\ \dot{q} \\ x \end{bmatrix} \tag{22}$$

To predict a flutter speed and frequency at a varying altitude, the following aspects need to be considered. When the altitude is changed, the corresponding atmospheric density will be changed as well. The change of the altitude also influences the speed of sound. If the speed of sound is obtained by a function of the altitude, the flight speed will be computed under a constant Mach number. Finally, all these variations are represented by functions of the altitude only.

5. Variation modeling with using uncertainty modeling method

5.1 Aerodynamic variation

The equation which governs an aerodynamic variation can be derived by extending Eq. (12), as follows:

$$\dot{x} = A_{Q_0}x + B_{Q_0}u_{new} \tag{23}$$

$$y = C_{Q_0}x + D_{Q_0}u_{new} \tag{24}$$

The refined Theodorsen's lift deficiency function, which includes the aerodynamic variation, is now written as

$$C(k)_{new} = \{-1 + b(\tfrac{1}{2}+a)+U\}\times C_{Q_0}x + D_{Q_0}u_{new} \tag{25}$$

$$u_{new} = \begin{bmatrix} u_{w_{new}} \\ u_{\theta_{new}} \end{bmatrix} \tag{26}$$

In the present paper, a variation existing in unsteady compressible aerodynamics is considered. Thus, the variations corresponding to both flight speed and atmospheric density are derived as follows. The present methodology for the aerodynamic variation modeling is different from that suggested in Ref. 2, where only a single parameter, which is the dynamic pressure, is varied.

$$\begin{aligned} u_{w_{new}} &= A_{Q_0}x + B_{Q_0}\{(U+W_U\Delta U)A^T\phi \\ &\quad -\dot{\eta} + b\left(\frac{1}{2}-a\right)A^T\dot{\phi}\} \end{aligned} \tag{27}$$

$$\begin{aligned} u_{\theta_{new}} &= A_{Q_0}x + B_{Q_0}b\left(\frac{1}{2}+a\right) \\ &\quad \{(U+W_U\Delta U)A^T\phi - \dot{\eta} + b\left(\frac{1}{2}-a\right)A^T\dot{\phi}\} \end{aligned} \tag{28}$$

$$U = (U_0 + W_U\Delta U) \tag{29}$$

$$\rho = (\rho_0 + W_\rho\Delta\rho) \tag{30}$$

Then, the robust aerodynamic forcing vector can be further derived as

$$\begin{aligned} \Xi_\omega &= -\pi(\rho_0+W_\rho\Delta\rho)b^2l\{[I]\ddot{\eta} + ba[A]^T\ddot{\phi}\} \\ &\quad -\pi(\rho_0+W_\rho\Delta\rho)b(U_0+W_U\Delta U)l2\{(C_{Q_0}x + D_{Q_0}\dot{\eta}) \\ &\quad -b[A]^T\dot{\phi} - 2b\left(\frac{1}{2}-a\right)[A]^T(C_{Q_0}x + D_{Q_0}\dot{\phi})\} \\ &\quad -\pi(\rho_0+\Delta W_\rho\rho)b(U_0+W_U\Delta U)^2l\{-2(C_{Q_0}x + D_{Q_0}\phi)\} \end{aligned} \tag{31}$$

$$\begin{aligned} \Xi_\theta &= -\pi(\rho_0+W_\rho\Delta\rho)b^2l\{ba[A]\ddot{\eta} + b^2\left(a^2+\frac{1}{8}\right)[I]\ddot{\phi}\} \\ &\quad -\pi(\rho_0+W_\rho\Delta\rho)b(U_0+W_U\Delta U)l\{2b\left(\frac{1}{2}+a\right) \\ &\quad (C_{Q_0}x + D_{Q_0}\dot{\eta})[A] + b^2\left(\frac{1}{2}-a\right)[I]\dot{\phi} \\ &\quad -2b^2\left(\frac{1}{2}-a\right)\left(\frac{1}{2}+a\right)(C_{Q_0}x + D_{Q_0}\dot{\phi})\} - \pi(\rho_0+W_\rho\Delta\rho) \\ &\quad b(U_0+W_U\Delta U)^2l(-b)(1+2a)(C_{Q_0}x + D_{Q_0}\phi) \end{aligned} \tag{32}$$

In modeling of the variation, input and output signals are arranged as follows.

$$z = \Delta w \tag{33}$$

In Equation (33), Δ is an uncertainty matrix which can be elaborated as

$$\Delta = \begin{bmatrix} 6\Delta U & 0 & 0 \\ 0 & 4\Delta\rho & 0 \\ 0 & 0 & 6\dfrac{1}{\Delta U} \end{bmatrix} \tag{34}$$

Aerodynamic variation coupling matrices can be represented as

$$\begin{bmatrix} Z_w \\ Q \end{bmatrix} = \begin{bmatrix} I & 0 \\ \bar{Q}_w & \bar{Q}_q \end{bmatrix} \begin{bmatrix} W_w \\ \dot{q} \\ q \end{bmatrix} \tag{35}$$

Then, the governing robust aeroelastic equation is arranged as

$$M\ddot{q} + Kq = Q_c\dot{q} + Q_kq + Q_Ax \tag{36}$$

For its corresponding state-space representation, Eqs. (23) and (36) need to be combined with each other, and

$$\begin{bmatrix} Z_w \\ Q_L \\ Q_M \\ \dot{x} \end{bmatrix} = [P] \begin{bmatrix} W_w \\ \dot{q} \\ q \\ x \end{bmatrix} \tag{37}$$

$$P = \begin{bmatrix} I_{16\times 16} \\ \bar{Q}_{L1\sim L21} \\ \bar{Q}_{M1\sim M21} \\ \bar{Q}_{A1\sim A21} \end{bmatrix} \tag{38}$$

In Eq. (38), $\bar{Q}_{L1\sim L21}$ and $\bar{Q}_{M1\sim M21}$ are lift and pitching moment coefficient, respectively. $\bar{Q}_{A1\sim A21}$ is an aerodynamic lag-state variable.

5.2 Mu (μ) method

Fig. 3 shows a closed-loop structure of the robust aeroelastic analysis established in the present paper. The mu method is used to analyze the worst case aeroelastic stability. Mu (μ) is a structured singular value of the system, and which is defined as

$$\mu(P) = \frac{1}{\min_{\Delta\in\mathbf{\Delta}} \{\bar{\sigma}(\Delta) : \det(I - P\Delta) = 0\}} \tag{39}$$

If mu is less than 1, then the system remains to be stable [7, 8]. In the previous application of Lind [2], the mu method was used in a robust analysis expressed in a single parameter only. However, as indicated in Eqs. (31) and (32) both the atmospheric density and flight speed are independent parameters in the present robust problem definition. Thus, the mu method is currently applied to a two-dimensional space spanned by both $\Delta\rho$ and ΔU. The worst case flutter condition can be extracted by scanning through a two-dimensional space, and the resulting robust flutter point will indicate a point which corresponds to the worst case atmospheric density and worst case flight speed simultaneously.

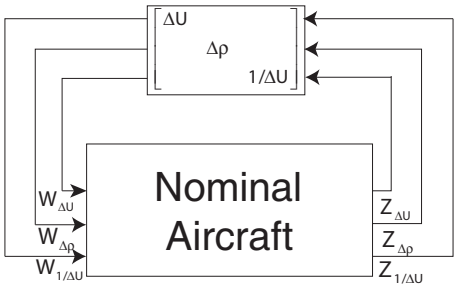

Fig. 3. Closed-loop structure for robust aeroelastic analysis.

It is specifically required to update the variation of aerodynamic state matrices $\Delta A, \Delta B, \Delta C, \Delta D$ in order to conduct an accurate robust aeroelastic analysis.

For a more accurate analysis, an update algorithm which uses a functional relationship among Mach number, flight speed, and the atmospheric density needs to be applied in the mu method. In more detail, the variation matrices $\Delta A, \Delta B, \Delta C, \Delta D$ need to be updated based on such functional relationship. However, such an update procedure is not included in the present analysis. Thus, if an initial condition is located far from the nominal flutter boundary, the robust analysis may not be capable of capturing an accurate flutter boundary.

5.3 Implementation of variation modeling

In Eqs. (29) and (30), the variation model is represented by the weighting matrix and ΔU and $\Delta\rho$, whose values are unity. The weighting matrix of aerodynamic state matrix is estimated based on the difference between the upper and lower boundary. Since the boundary of altitude and Mach number variation is prescribed, the boundary of the flight speed can be obtained. Thus, the weighting matrix is represented as

$$W_\rho = \rho_{upper} - \rho_{low} \tag{40}$$

$$W_U = U_{upper} - U_{low} \tag{41}$$

In the present variation model, the upper and lower bound of the altitude is prescribed as 80,000 and 20,000 ft, respectively. Thus, the upper and lower bound of the atmospheric density can be obtained from those prescribed for the altitude. Then, the flight speed boundary is obtained from the altitude and Mach number boundaries. For Mach number variation, the weighting matrix of aerodynamic state matrix is represented as

$$W_A = A_{ij,upper} - A_{ij,lower} \tag{42}$$

$$W_B = B_{ij,upper} - B_{ij,lower} \tag{43}$$

$$W_C = C_{ij,upper} - C_{ij,lower} \tag{44}$$

$$W_D = D_{ij,upper} - D_{ij,lower} \tag{45}$$

The lower and upper bound of Mach number is assumed to be 0.5 and 0.76, respectively.

6. Numerical results

In the present paper, a numerical analysis is conducted by using a three-dimensional rectangular wing geometry which was used by Goland [4]. Table 1 summarizes properties of the three-dimensional cantilevered wing.

6.1 Result of the nominal aircraft

6.1.1 Natural frequency analysis

Table 2 shows the results for the natural frequency estimation of the present wing. First, natural frequencies are analyzed for two different cases, one with a static imbalance S and the other without S. Table 2 also presents the comparison of the two results. The present method without considering a static imbalance shows similar results with the general uncoupled beam analysis.

6.1.2 DLM analysis result

A three-dimensional wing with aspect ratio of 20, is analyzed to extract the corresponding two-dimensional airfoil aerodynamic forces. The aspect ratio of panels used in the DLM computation is approximately 2. The lift deficiency function is obtained by DLM at a given flight Mach number, and the nominal and robust flutter stability boundaries are predicted for the corresponding Mach number. Such approach signifies that the altitude is varied and the dynamic pressure is related to the flight speed and air density.

The complex two-dimensional aerodynamic forces

Table 1. Characteristics of goland's wing [4].

Characteristics			
Wing Span	20*ft*	Static Imbalance (ξ)	0.447 *slug/ft*
Chord length	6*ft*	EI	$m \times 31.7 \times 10^6$ $lb \cdot ft^3/slug$
Radius of Gyration	25% Chord	GJ	$I \times 1.23 \times 10^6$ $lb \cdot ft/slug$
Spanwise Elastic Axis	33% Chord	Mass Moment of Inertia (I)	1.943 $lb \cdot ft^2/ft$
Center of Gravity	43% Chord	Mass of Unit Length (m)	0.743 *Slug/ft*
Semi Chord	3*ft*		

Table 2. Natural frequency result (rad/sec).

	1st Bending	1st Torsion	2nd Bending	2nd Torsion
Goland [4]	50.0	87.0	-	-
Present Method (With S)	47.8	91.6	333.9	249.0
Present Method (Without S)	48.5	87.1	310.1	261.3
Uncoupled Beam analysis	49.5	87.1	308.4	261.3

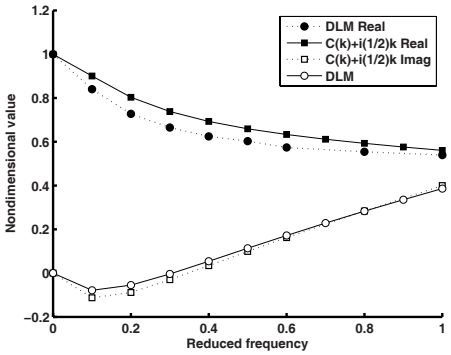

Fig. 4. Complex indicial aerodynamic forces due to pitching obtained by DLM.

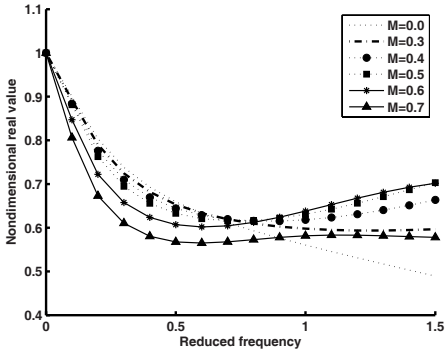

Fig. 5. Non-dimensionalized real part in indicial lift vs. Mach No.

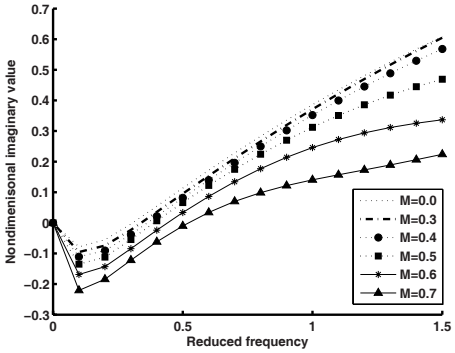

Fig. 6. Non-dimensionalized imaginary part in indicial lift vs. Mach No.

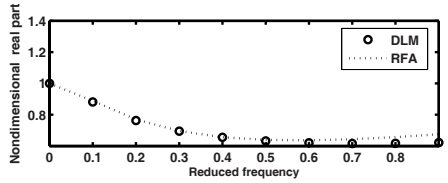

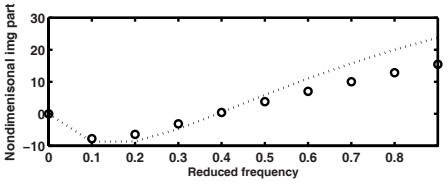

(a) M=0.5

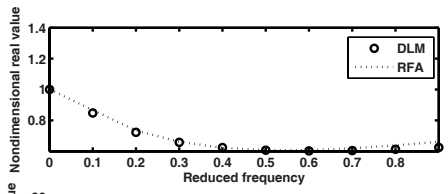

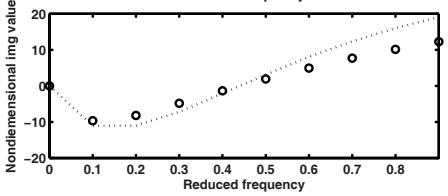

(b) M=0.6

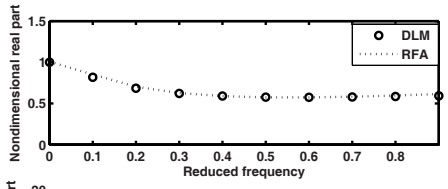

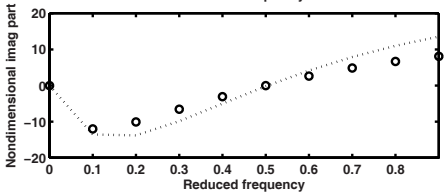

(c) M=0.7

Fig. 7. Comparison between DLM and RFA for Mach = 0.5, 0.6, and 0.7.

due to a pitching motion of the wing are obtained by the present DLM analysis, In Fig. 4, one of the pre sent DLM results corresponding to the case of Mach number 0, is compared with the Theodorsen's lift deficiency function [5, 12]. As shown in the figure, there is a good agreement between the two results. The real and imaginary parts as functions of flight Mach number are plotted separately in more detail in Figs. 5 and 6. The present DLM result for the unsteady lift shows decreasing and increasing pattern, respectively, for its real and imaginary part. In RFA, a number of iterative fitting procedures are conducted regarding the pole and zero values to match between the DLM analysis and its approximation. Thus the RFA result needs to be compared with those originally obtained by DLM analysis.

Fig. 7 shows a comparison between the DLM analysis and the corresponding RFA results for Mach number 0.5, 0.6, and 0.7, respectively. It can be seen that they exhibit a good agreement within the interval of the reduced frequencies of interest.

Table 3. Validation of the flutter estimation results.

	Flutter Speed (ft/sec)	Flutter Frequency (rad/sec)
Goland [4]	575	69
Brown [13]	574	70
Present Quasi-Steady	529	70
Present Unsteady	562	71.1

6.1.3 Nominal flutter estimation result

When a typical aircraft performs its designated mission, its altitude may be changed significantly. In the present paper, a nominal aircraft is assumed to conduct a flight at a varying altitude. The nominal aeroelastic validation results are summarized in Table 3. If altitude is prescribed to be a changing value, the atmospheric density will be influenced. The present results are obtained at 20,000 ft above sea level. The nominal aeroelastic analysis results are summarized in Table 4.

The present nominal flutter estimation is performed for varying atmospheric density for two different aerodynamic models. The first case considers the full blown unsteady aerodynamic forces and the other case considers only the circulatory part in unsteady aerodynamic force.

The results corresponding to the first case are obtained for an altitude of 20,000 ~ 90,000 ft above sea level. An initial flight Mach number is assumed to be 0.5, 0.6, 0.7, 0.74, 0.76, respectively, and Theodorsen's lift deficiency function is approximated for the given Mach numbers. The results for the second case are obtained for an altitude of 20,000 ~ 80,000 ft above sea level. An initial flight Mach number is assumed to be 0.5, 0.6, 0.7, since the flutter speed is

Table 4. Nominal aeroelastic stability analysis results.

Nominal Flutter Results (full blown unsteady)					
Mach Number	Flutter Speed (ft/sec)	Flutter Frequency (rad/sec)	Flutter Dynamic Pressure (slug/ft^2· sec)	Corresponding Altitude (ft)	Corresponding Atmospheric Density (slug/ft^3)
0.5	522.4	72.5	167.7	20,893	0.0012
0.6	610.73	79.4	97.09	43,660	$5.02 \cdot 10^{-4}$
0.7	701.71	85.2	71.69	56,648	$2.91 \cdot 10^{-4}$
Nominal Flutter Results (Considering only the circulatory part)					
Mach Number	Flutter Speed (ft/sec)	Flutter Frequency (rad/sec)	Flutter Dynamic Pressure (slug/ft^2· sec)	Corresponding Altitude (ft)	Corresponding Atmospheric Density (slug/ft^3)
0.5	528.2	75.8	177.13	19,981	0.0013
Difference with Full unsteady	+1.18%	+5.0%	+5.7%	-4.3%	+7.6%
0.6	617	83.2	102.2	42,962	$5.368 \cdot 10^{-4}$
Difference with Full unsteady	+1.13%	+4.5%	+5.08%	-1.59%	+6.34%
0.7	710	95.5	79.7	54,946	$3.16 \cdot 10^{-4}$
Difference with Full unsteady	+1.26%	+10.5%	+10.05%	-3%	+7.9%

expected to be between Mach 0.5 ~ 0.7. From RFA, the state-space form is obtained and the aeroelastic coupling matrix is constructed. For verification of the nominal flutter analysis results, the present nominal flutter results are compared with the previous analytical results. Variation of the atmospheric density influences the speed of sound. Since the speed of sound is a function of altitude, the flight speed will be defined for a constant Mach number for a certain altitude. Finally, the entire formulation is represented as a function of an altitude only. In the present paper, flutter speed and frequency prediction for a nominal aircraft are conducted by varying the altitude and under a constant Mach number. The nominal flutter speed results for the first case are obtained to be 1.13 ~ 1.26% lower than those for the second case. The nominal flutter frequencies are obtained to be 4.5 ~ 10% lower value than those only with circulatory part.

As stated earlier, the present results are obtained for 0 different atmospheric densities. This indicates that the altitude of the aircraft exhibits different numerical values. At each flutter boundary, the atmospheric density decreases as the altitude increases, and the corresponding dynamic pressure decreases as the flight Mach number increases.

6.2 Result of the robust aeroelastic stability analysis

To conduct a robust flutter stability analysis, variation boundaries for the flight Mach number need to be estimated in advance. In the present paper, the lower and upper bounds are estimated regarding the flight speed and atmospheric altitude, and then the corresponding weighting values are obtained as follows.

$$W_\rho = 5.9379 \times 10^{-4} \ \ (\text{slug}/\text{ft}^3) \tag{46}$$

$$W_U = 108.87 \ \ (\text{ft}/\text{sec}) \tag{47}$$

$$W_A = \begin{bmatrix} -16.4711 & -44.57 & -6.47 \\ 1 & 0 & 0 \\ 0 & 1 & 0 \end{bmatrix} \tag{48}$$

$$W_B = \begin{bmatrix} 1 \\ 1 \\ 1 \end{bmatrix} \tag{49}$$

$$W_C = [-9.0672 \quad -9.0672 \quad -9.0672] \tag{50}$$

$$W_D = 0.2439 \tag{51}$$

Then, the robust aeroelastic coupling matrices are constructed and the mu method is used for the worst case analysis. The present robust analysis result is

Table 5. Robust aeroelastic stability analysis results.

(a) M=0.5

Robust Flutter Analysis							
Initial Mach	Initial Altitude (ft)	Flutter Speed (ft/sec)	Flutter Mach	Flutter Frequency (rad/sec)	Flutter Dynamic Pressure (slug/ft^2· sec)	Corresponding Altitude (ft)	Corresponding Atmospheric Density (slug/ft^3)
0.5	40,000	524.3	0.511	90.96	92.22	37,408	$6.709 \cdot 10^{-4}$
	Difference with Nominal Result	-0.76%	+2.2%	+25.5%	-47.92%	+87.17%	-48.39%
	30,000	522.6	0.505	90.66	124.52	29,336	$9.12 \cdot 10^{-4}$
	Difference with Nominal Result	-1.02%	+1.0%	+25.0%	-29.68%	+47.5%	-29.84%
	25,000	525.2	0.504	90.48	149.28	24,560	$1.082 \cdot 10^{-3}$
	Difference with Nominal Result	-0.57%	+0.8%	+24.8%	-15.7%	+23.50%	-16.76
	20,000	529.0	0.506	90.32	179.34	19,666	$1.281 \cdot 10^{-3}$
	Difference with Nominal Result	+0.2%	+1.2%	+24.5%	-1.26%	-1.10%	-1.46%

(b) M=0.6

Robust Flutter Analysis							
Initial Mach	Initial Altitude (ft)	Flutter Speed (ft/sec)	Flutter Mach	Flutter Frequency (rad/sec)	Flutter Dynamic Pressure (slug/ft^2· sec)	Corresponding Altitude (ft)	Corresponding Atmospheric Density (slug/ft^3)
0.6	60,000	606.0	0.605	91.35	51.33	57,497	$2.79 \cdot 10^{-4}$
	Difference with Nominal Result	-1.8%	+0.8%	+9%	-49.67%	+33.8%	-47.9%
	55,000	604.3	0.601	91.26	58.85	54,503	$3.22 \cdot 10^{-4}$
	Difference with Nominal Result	-2.1%	+0.16%	+9.6%	-42.3%	+26.86%	-40%
	50,000	625.9	0.616	91.15	92.52	45,965	$4.72 \cdot 10^{-4}$
	Difference with Nominal Result	+1.4%	2.66%	+9.5%	9.47%	+6.98%	-12.1%
	45,000	628.6	0.616	91.03	110.35	41,967	$5.58 \cdot 10^{-4}$
	Difference with Nominal Result	+1.3%	2.66%	+9.4%	+7.63%	-2.3%	+8%

(c) M=0.7

Robust Flutter Analysis							
Initial Mach	Initial Altitude (ft)	Flutter Speed (ft/sec)	Flutter Mach	Flutter Frequency (rad/sec)	Flutter Dynamic Pressure (slug/ft^2· sec)	Corresponding Altitude (ft)	Corresponding Atmospheric Density (slug/ft^3)
0.7	70,000	698.7	0.705	91.47	42.81	66,619	$1.75 \cdot 10^{-4}$
	Difference with Nominal Result	-1.6 %	+0.71%	-4.21%	-46.28%	+17.52%	-44.62%
	65,000	696.4	0.701	91.40	47.81	64,424	$1.97 \cdot 10^{-4}$
	Difference with Nominal Result	-1.9%	+0.14%	-4.2%	-40.01%	17.24%	-37.65%
	60,000	709.3	0.708	91.31	70.76	57,366	$2.81 \cdot 10^{-4}$
	Difference with Nominal Result	-0.1%	+1.14%	-3.88%	-11.2%	+4.4%	-11.07%
	55,000	710.1	0.705	91.21	84.88	53,570	$3.37 \cdot 10^{-4}$
	Difference with Nominal Result	0%	-0.71%	-3.98	+6.4%	-2.5%	+6.6%

based on the two-dimensional lift curve slope. For the robust flutter analysis, an initial flight Mach number and altitude are selected with respect to three Mach numbers. The first case is an initial altitude to be 20,000 ft, 25,000 ft, 30,000 ft and 40,000 ft. This corresponds to an initial Mach number of 0.5. The second case is 45,000 ft, 50,000 ft, and 60,000 ft corresponding to the initial Mach number 0.6. The third case is assumed to be 55,000 ft, 60,000 ft, 65,000 ft, and 70,000 ft at initial Mach number 0.7. The results from the present nominal analysis and those from the robust flutter analysis are summarized in Table 5.

The robust flutter analysis results are compared with those from the nominal flutter analysis, both of which currently consider only circulatory terms in unsteady aerodynamics. Among the presently contracted flight envelope, a certain flight condition point is located farthest from the nominal flight envelope, and such point is considered to be the worst flutter condition, which is the target of the present paper.

According to the present procedure, the corresponding worst case flutter speed is obtained for each case. For the first case, the robust flutter speed is 524 ~ 529 ft/sec at each initial flight altitude, and this result is -0.1 ~ 0.8% smaller than that for the nominal analysis under the same flight Mach number. The worst case flutter frequency is 90.32 ~ 90.96 rad/sec, flutter altitude 19,666~37,408ft, and the corresponding dynamic pressure is 92.2 ~ 179.34 slugs/ft^3 obtained at each initial altitude at initial Mach number 0.5The robust flutter frequencies are 19.9 ~ 20% higher than the nominal frequency and the robust altitudes are higher by -1.57 ~ 87.2 %. Furthermore, Mach number result shows a slight change of approximately 0.506 ~ 0.511 and this result presents differences, 1.2 ~ 2.2% from the nominal flutter Mach number. For the second case, the robust flutter speeds are 606 ~ 628.6 ft/sec and these values are -3.5 ~ 1.8 % smaller than those for the nominal analysis under the initial flight Mach number 0.6 and each initial flight altitude. The worst case flutter frequencies are 91.03 ~ 91.35 rad/sec, flutter altitude 41,697 ~ 57,497 ft, and the corresponding dynamic pressures are 51.33 ~ 110.35 slugs/ft^3 at each initial altitude The variation result of Mach number shows a slight change of approximately, 0.605 ~ 0.616. This result represents slight differences, 0.83 ~ 2.66% from nominal flutter Mach number.

For the third case, the robust flutter speeds are 698.7 ~ 710 ft/sec and these values are 1.59 ~ 0 % smaller than those for the nominal analysis under the initial flight Mach number 0.7. The worst case flutter frequencies are 91.21 ~ 91.47 rad/sec, flutter altitudes are 53,570 ~ 66,619 ft, and the corresponding dynamic pressures are 42.81 ~ 84.88 slugs/ft^3. The variation result of Mach number shows approximately, 0.701 ~ 0.708. These results present slight differences, 0.14~1.14% from nominal Mach number. The meaning of the worst case flutter boundary is illustrated in Fig. 8. As shown in Figure 8, the worst case flutter boundary is obtained by predicting the nearest point from the initial condition.

The above results present a reasonable trend with respect to Mach number and atmospheric density. In the present robust result, the worst case flutter boundaries are shown to be more conservative flutter speed, dynamic pressure, and flutter altitude than those of the nominal flutter analysis. However, when the initial condition is located far from the nominal flutter boundary, the worst case flutter boundaries provide more conservative results.

The present analysis considers a varying Mach number, which is given from a variation of the flight altitude. However, the functional relationship among the variables is not accounted during the present mu iteration, and the boundary of each variation is prescribed. Thus, the mu method cannot predict the nearest point if the initial flight state is accidentally located far from the nominal flutter boundary.

In the present preliminary robust analysis, such variation of the aerodynamic state-space matrices is approximately implemented by RFA procedure. The variation in the flight speed and that due to atmospheric density are reflected in the weighting matrices,

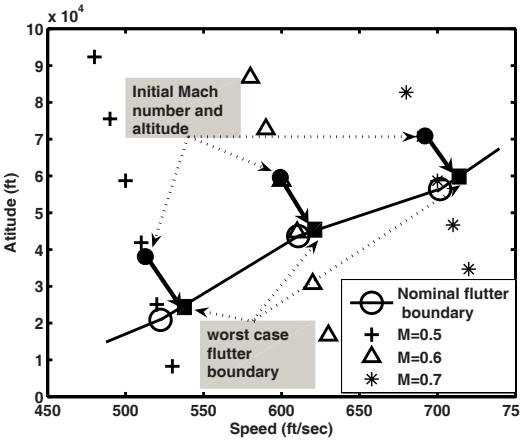

Fig. 8. The worst case flutter boundary.

such as ΔU , $\Delta\rho$. Such an approximate procedure allows prediction of the worst case flutter speed with respect to the given Mach number and atmospheric density.

7. Conclusion

A brand new robust aeroelastic analysis methodology is proposed including a variation existing in unsteady compressible aerodynamics. Such a variation is assumed in the model to account for varying Mach effects in a given flight envelope. In the present approach, a three-dimensional wing also experiences varying atmospheric density and dynamic pressure due to changes in the flight speed and altitude. For a nominal aircraft, a traditional aerodynamic analysis based on the two dimensional Theodorsen's lift deficiency function is used. DLM analysis is then conducted to extract more accurate unsteady compressible aerodynamic forces acting on the three-dimensional wing. After that, RFA is conducted to compute the transfer function corresponding to Theodorsen's lift deficiency function and then it is transferred to a space-state form. For a robust aeroelastic analysis, a range of the aerodynamic variation is quantified by specifying the lower and upper limits in the RFA coefficients resulting from the change in the Mach number. On the other hand, the functional relation between the altitude and atmospheric density is exactly accounted by the match point method. Then, a worst case flutter stability boundary is found by using the mu method and compared with those obtained from the nominal stability analysis at Mach number 0.5, 0.6, 0.7, respectively. The nominal flutter analysis is performed in two cases, which considers full blown unsteady aerodynamics and only the circulatory part. The worst case flutter boundary results are shown 1.2% ~2.1% lower than nominal flutter boundary at each initial Mach condition 0.5, 0.6, and 0.7. Since the exact relation between the Mach, flight speed, and the altitude is not considered during the mu analysis, the current mu method cannot predict the nearest point in case the initial flight state is located far from the nominal flutter boundary. However, the present analysis results show a reasonable trend for the worst case flutter prediction. In the future, a more accurate method will be investigated, such as an iterative method in frequency domain based on three-dimensional generalized aerodynamic forces for the worst case problem.

Acknowledgments

This work was supported by the Korea Research Foundation Grant funded by the Korean Government (MOEHRD, Basic Research Promotion Fund) (KRF-2006-331-D00086). This work was also supported by the City of Seoul Fellowship, Korea.

Nomenclature

M	:	Mass matrix
K	:	Stiffness matrix
F_G	:	Aerodynamic force matrix
A_M	:	Aerodynamic mass matrix
A_c	:	Aerodynamic damping matrix
A_G	:	Aerodynamic lag state matrix
A_K	:	Aerodynamic stiffness matrix
q	:	Generalized coordinate
η	:	Bending modal coordinate
θ	:	Torsion modal coordinate
Ψ	:	Bending mode shape
Θ_i	:	Torsion mode shape
A_{ij}	:	Coupling modal matrix
B_{ij}	:	Bending mode frequency coefficient matrix
T_{ij}	:	Torsion mode frequency coefficient matrix
Ξ_ω	:	Generalized aerodynamic lift
Ξ_θ	:	Generalized aerodynamic pitching moment
L'	:	Lift for the two-dimensional airfoil
$M_{1/4}$	:	Pitching moment of the two-dimensional airfoil about a 1/4 chord point
$C(k)$	:	Theodorsen's lift deficiency function
W_U, W_ρ, $W_{1/U}$	:	Uncertainty weighting scalar value
$C(k)_{new}$	:	Uncertainty in Theodorsen's function
b	:	Semi-chord
S	:	Structural imbalance
EI	:	Bending stiffness coefficient
GJ	:	Torsion stiffness coefficient
m	:	Mass per span wise unit length
x_θ	:	Distance between C.G and E.A
$\bar{\sigma}$	:	Singular value
Δ	:	Uncertainty matrix
P	:	Uncertainty of the coupled system matrix
U_0	:	Flight speed at initial level

ρ_o : Atmospheric density at initial level
Z_w : Output of the uncertainty matrix
W_w : Weighting for the uncertainty matrix
x : Aerodynamic lag state
η : Bending mode shape function
ϕ : Torsion mode shape function
α : Bending coefficient in the mode shape
β : Torsion coefficient in the mode shape
A_Q, B_Q, C_Q, D_Q : Nominal aerodynamic state matrix

References

[1] E. Livne, Future of Airplane Aeroelasticity, *Journal of Aircraft*. 40 (6) (2003) 1066-1092.
[2] R. Lind, Match-Point Solutions for Robust Flutter Analysis, *Journal of Aircraft*. 39 (1) (2002) 91-99.
[3] D. Borglund, The μ-k Method for Robust Flutter Solutions, *Journal of Aircraft*. 41 (5) (2004) 1209-1216.
[4] M. Goland, The Flutter of a Uniform Cantilever Wing, *Journal of Applied Mechanics*. 12 (4) (1945) A197- A208.
[5] K. C. Hall, Eigenanalysis of Unsteady Flows about Airfoils, Cascades, and Wings, *AIAA Journal*. 32 (12) (1994) 2426-2432.
[6] D. H. Hodges, *Introduction to Structural Dynamics and Aeroelasticity*, Cambridge University Press, New York, USA. (2002).
[7] K. Zhou, *Essentials of Robust Control*, Prentice Hall, Upper Saddle River, N.J. USA. (1998).
[8] R. Lind and M. Brenner, *Robust Aeroservoelastic Stability Analysis*, Springer, London, UK. (1999).
[9] R. L. Bisplinghoff, H. Ashley and R. L. Halfman, *Aeroelasticity,* Addison Wesley, Cambridge, MA, (1955).
[10] B. P. Danowsky and F, K. Chavez, Formulation of an Aircraft Structural Uncertainty Model for Robust Predictions, *Proceedings of the 45th AIAA/ASME/ASCE/AHS/ASC Structures, Structural Dynamics & Materials Conference*, (2004) 1-15.
[11] M. A. Blair, A Compilation of the Mathematics Leading to the Doublet Lattice Method, *Air Force Wright Laboratory, Dayton, OH, WL-TR-92-3028*, (1992).
[12] T. Theodorsen, General Theory of Aerodynamic Instability and the Mechanism of Flutter, *NACA Report 496*, (1934).
[13] E. L. Brown, *Integrated Strain Actuation in Aircraft with Highly Flexible Composite Wing*, Sc. D. Thesis, Mechanical Engineering, Massachusetts Institute of Technology, Cambridge MA, June. (2003).

ChanHoon Chung received M.S degree in Mechanical Engineering from Korea University in 2004. Since 2005, he has been a Ph.D student at the School of Mechanical and Aerospace Engineering in Seoul National University. His research interests include robust aeroelasticity and aeroservoelasticity.

SangJoon Shin received S.M. and Ph.D. degrees in Aeronautics and Astronautics from Massachusetts Institute of Technology in 1999 and 2001, respectively. During 1991 – 1996, he worked at the Helicopter Systems Department, Korean Agency for Defense Development. During 2001- 2003, he worked at the Department of erospace Engineering, University of Michigan, Ann Arbor. Since 2003, he has been a professor at the School of Mechanical and Aerospace Engineering in Seoul National University. His research interests include aeroelasticty, rotorcraft dynamics, and smart structures.

Taehyoun Kim earned a Ph.D. in Aeronautics and Astronautics from Massachusetts Institute of Technology in 1992. Since 1996 he has worked in Loads and Dynamics Group of Boeing Commercial Aircraft, Seattle, Washington, USA. Prior to joining the Boeing Company he worked in Computational Mechanics Laboratory at Georgia Institute of Technology. Since 2005, he has been teaching a short course, "Computational Methods in Aeroelasticity" at SDM Conference, Boeing Ed Wells, National Aerospace Laboratory in India, and NASA Langley. Dr. Kim's specialties are aeroservoelasticity/structural dynamics, computational and experimental methods in aeroelasticity, system identification and model reduction of large-scaled dynamic systems, and composite structures.